

# Airborne hyperspectral remote sensing applied to determine the texture of a Cambisol in the Chapada do Apodi, Ceará<sup>1</sup>

## Sensoriamento remoto hiperespectral aerotransportado aplicado na determinação da textura de um Cambissolo da Chapada do Apodi-CE

Eurileny Lucas de Almeida<sup>2\*</sup>, Marcio Regys Rabelo de Oliveira<sup>3</sup>, Odílio Coimbra da Rocha Neto<sup>3</sup>, Luís Clenio Jário Moreira<sup>4</sup> and Adunias dos Santos Teixeira<sup>3</sup>

**ABSTRACT** - Texture is of great importance in soil management, as it strongly influences the physical, hydraulic and chemical behaviour of soils. It is therefore necessary to determine texture, with the spectral band ratio being a fast and precise alternative method for this purpose. The aim of this study was to evaluate the use of spectral data, acquired by the ProSpecTIR-VS airborne sensor with a spatial resolution of 1 m, in selecting two bands for building a Normalised Difference Index that allows the textural attributes of the soil to be estimated, besides preparing a texture map of the soil in the image. Sixty-four samples were collected from several areas inserted in the Jaguaribe-Apodi irrigated perimeter, which is located in the Chapada do Apodi, in the Lower Jaguaribe Basin, where the predominant soil classes are Cambisols. The samples were collected from exposed soil, based on the hyperspectral images of the ProSpecTIR-VS airborne sensor. The Normalised Difference Index (NDI) was constructed, carrying out all possible normalised band ratios, with the best indices selected based on the coefficient of determination ( $R^2$ ). The most promising results for  $R^2$  were obtained when estimating sand in the 1045 and 1323 nm bands, with an  $R^2$  of 0.5. The low values for  $R^2$  can be explained by interference in the spectral response from materials on the soil surface, such as crop residue, gravel and vegetation. Preparing the sand map using the best model resulted in 82.1% of the pixels having values between 20 and 60% sand, falling between the minimum and maximum sand content of the soil samples.

**Key words** - Precision agriculture. Reflectance spectroradiometry. SpecTIR-VS sensor.

**RESUMO** - A textura tem grande importância no manejo dos solos, pois influencia fortemente o comportamento físico-hídrico e químico dos solos. É necessário, portanto, a determinação de tal textura, sendo a razão de bandas espectrais, uma alternativa rápida e precisa para este fim. O objetivo deste trabalho foi avaliar o uso de dados espectrais, adquiridos pelo sensor aerotransportado ProSpecTIR-VS, com resolução espacial de 1 m, na seleção de duas bandas para composição de um Índice por Diferença Normalizada, que permita estimar os atributos texturais do solo, além de elaborar o mapa textural do solo na imagem. Foram coletadas 64 amostras em áreas inseridas no perímetro irrigado Jaguaribe-Apodi, que se localiza na Chapada do Apodi, Bacia do Baixo Jaguaribe, cujas classes predominantes são Cambissolos. As amostras foram coletadas em solo exposto, tendo como base as imagens hiperespectrais do sensor aerotransportado ProSpecTIR-VS. O Índice por Diferença Normalizada (NDI) foi construído, realizando-se todas as possíveis relações normalizadas de bandas e os melhores índices foram selecionados com base no coeficiente de determinação ( $R^2$ ). Os resultados mais promissores de  $R^2$  foram obtidos na estimativa da areia, com as bandas 1045 e 1323 nm, com  $R^2$  de 0.5. Os baixos valores de  $R^2$  podem ser explicados pela interferência na resposta espectral por materiais que estavam na superfície do solo, como resto de cultura, cascalho e da vegetação. A elaboração do mapa de areia utilizando o melhor modelo resultou em 82.1% dos pixels com valores entre 20 e 60% de areia, enquadrando-se entre mínimo e máximo dos teores de areia das amostras de solos.

**Palavras-chave** - Agricultura de precisão. Espectrorradiometria de reflectância. Sensor SpecTIR-VS.

DOI: 10.5935/1806-6690.20210023

Editor-in-Article: Prof. Adriel Fonseca - adrielff@gmail.com

\*Author for correspondence

Received for publication 11/03/2020; approved on 21/10/2020

<sup>1</sup>Parte da Tese do primeiro autor, apresentado ao Programa de Pós-Graduação em Ciência do Solo da Universidade Federal do Ceará

<sup>2</sup>Instituto Federal de Educação, Ciência e Tecnologia Baiano – *Campus* Bom Jesus da Lapa, Bom Jesus da Lapa-BA, Brasil, eurileny@gmail.com (ORCID ID 0000-0002-2582-1521)

<sup>3</sup>Departamento de Engenharia Agrícola, Universidade Federal do Ceará/UFC, Fortaleza-CE, Brasil, marciorregys01@gmail.com (ORCID ID 0000-0002-1150-1498), odilioneto@gmail.com (ORCID ID 0000-0002-5772-8348), adunias@ufc.br (ORCID ID 0000-0002-1480-0944)

<sup>4</sup>Instituto Federal de Educação, Ciência e Tecnologia do Ceará, *Campus* Limoeiro do Norte, Limoeiro do Norte-CE, Brasil, cleniojario@gmail.com (ORCID ID 0000-0001-9918-9744)

## INTRODUCTION

Soil texture, which represents the relative proportions of sand, silt and clay particles (BRADY; WEIL, 2013), is of great importance in soil management, as it affects the physical, hydraulic and chemical behaviour of the soil. However, obtaining textural data via particle-size analysis when it is necessary to prepare thematic maps of sand or clay, for example, is costly in large areas, given that soil texture usually displays high spatial variability.

Techniques that estimate this soil attribute more quickly and less invasively are therefore of great value. It is here that reflectance spectroradiometry is seen as a viable alternative for estimating various soil attributes, including texture (CASA *et al.*, 2013; CASTALDI *et al.*, 2014, 2016; CEZAR *et al.*, 2012; LIAO *et al.*, 2013), as the technique is fast and non-destructive, especially when using aerial sensors.

One of the ways to use the spectral data of soils is through the division or ratio between bands using a non-linear mathematical operation. The principal aim is to highlight the spectral differences in a pair of bands that characterise certain features of the target spectral signature curve (NANNI; DEMATTÊ, 2006; RIBEIRO; SILVA; SILVA, 2016; VIÑA *et al.*, 2011), also called an index.

Hyperspectral data, which are characterised as data collected in narrow and continuous bands of the spectrum, have greater potential for preparing indices than do multispectral data (broad bands), as they enable the acquisition of far more detailed information about the target, such as the physical properties of the soil. This data can be obtained at different levels of acquisition, for example, the ProSpecTIR-VS airborne sensor (SpecTIR Advanced Hyperspectral Solutions), which operates in 357 spectral bands in the visible (VS), near infrared (NIR) and shortwave infrared (SWIR), to which Brazil gained access in 2010, when the Brazilian company FotoTerra® entered into a technological partnership with the American company SpecTIR®. Since then, numerous studies in various areas have been carried out using data from this sensor (AMARAL *et al.*, 2015, 2018; ROCHA NETO *et al.*, 2017; SANCHES; SOUZA FILHO; KOKALY, 2014; STREHER *et al.*, 2014).

Given the above, the aim of this study was to apply spectral data, acquired by the ProSpecTIR-VS sensor, to selecting bands for building a Normalised Difference Index capable of estimating the textural attributes of the soil, as well as prepare a texture map of the soil in the image.

## MATERIAL AND METHODS

### Study area

The study was carried out in several areas inserted in the Jaguaribe-Apodi irrigated perimeter, which is located

in the Chapada do Apodi, in the Lower Jaguaribe Basin (Figure 1). In general, the Chapada do Apodi consists of cretaceous sediments of the Jandaíra and Açú formations, with the predominant occurrence of Cambisols (JACOMINE; ALMEIDA; MEDEIROS, 1973). In the areas of flat relief there are eutrophic Cambisols, derived from carbonate rocks of the Apodi Group comprising high-activity clay of a clayey texture. These soils have high natural fertility and great potential for agricultural use (GATTO, 1999).

According to the Köppen classification, the climate in the region is type BSw'h', characterised by an average annual temperature of 28.5°C, with a minimum of 22°C and maximum of 35°C. The average annual rainfall is 772 mm, with irregular rainfall over the years (AGÊNCIA DE DESENVOLVIMENTO DO ESTADO DO CEARÁ, 2011).

### ProSpecTIR-VS airborne sensor

On 24 May 2015, hyperspectral images were obtained from the ProSpecTIR-VS airborne sensor through a technological partnership with the Brazilian company FotoTerra® and resources from the National Council for Scientific and Technological Development (CNPq), via the National Institute for Salinity Science and Technology (INCT-Sal). Table 1 shows the characteristics of the sensor used to obtain the hyperspectral images.

Transformation of the spectral data (Digital Number-DN) into surface reflectance, applying atmospheric correction, was carried out by the FotoTerra® company using a method based on the MODTRAN-4 radiative transfer model (Moderate Resolution Atmospheric Transmission). The respective GLT files (Geographic Lookup Table) provided by the company were used for georeferencing the hyperspectral images.

### Collecting soil samples

Sixty-four deformed soil samples were collected at a depth of 0-10 cm, with the sampling points located in areas of exposed soil, based on the images acquired with the ProSpecTIR-VS airborne sensor. Particle size analysis was carried out using the pipette method as described by Teixeira *et al.* (2017), to obtain the sand, silt and clay content.

The soil samples were collected from November 2017 to February 2018; the following procedure was carried out to assist in allocating the points: I - the NDVI (Normalised Difference Vegetation Index) was calculated using the spectral data acquired by the ProSpecTIR-VS airborne sensor; II - using map algebra with pixel grouping, pixels with an NDVI value of less than 0.3 were separated, this value being considered for exposed soils, as observed by Rocha Neto *et al.* (2017), and III - pixels with an NDVI of less than 0.3 were plotted on a Google Earth® image using the QGIS® 2.18 software (Figure 2), this last step being necessary to help locate the points when collecting in the field.

**Figure 1** - Location of the study area

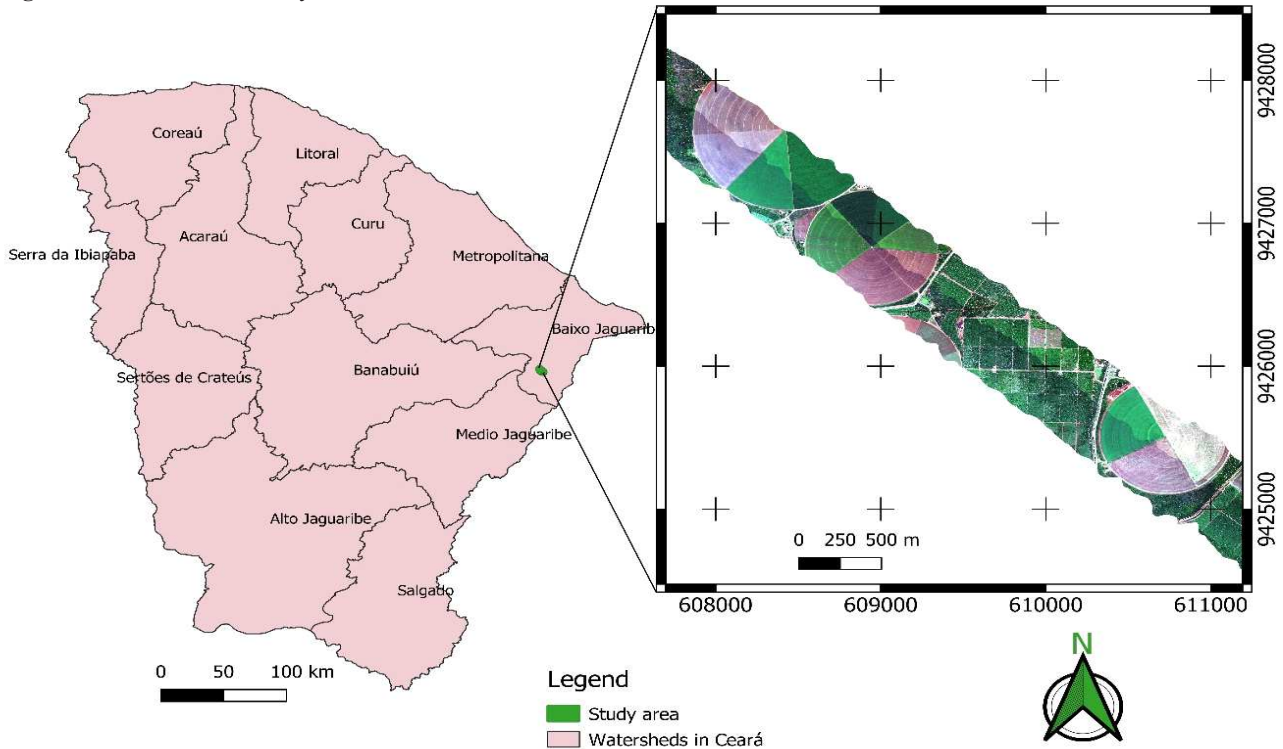
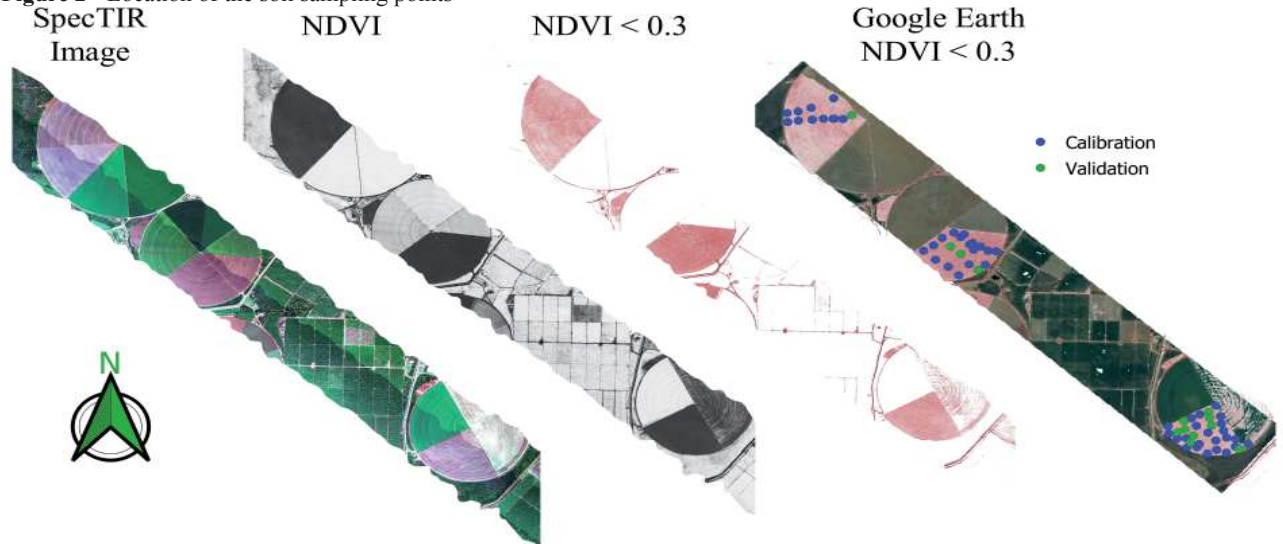


**Table 1** - Characteristics of the hyperspectral sensor

Sensor	ProSpecTIR-VS
Spectral band	400 a 2500 nm
Spectral resolution	5 nm
Number of bands	357
Spatial resolution*	1 metre

\*Flight plan projected for a spatial resolution of 1m

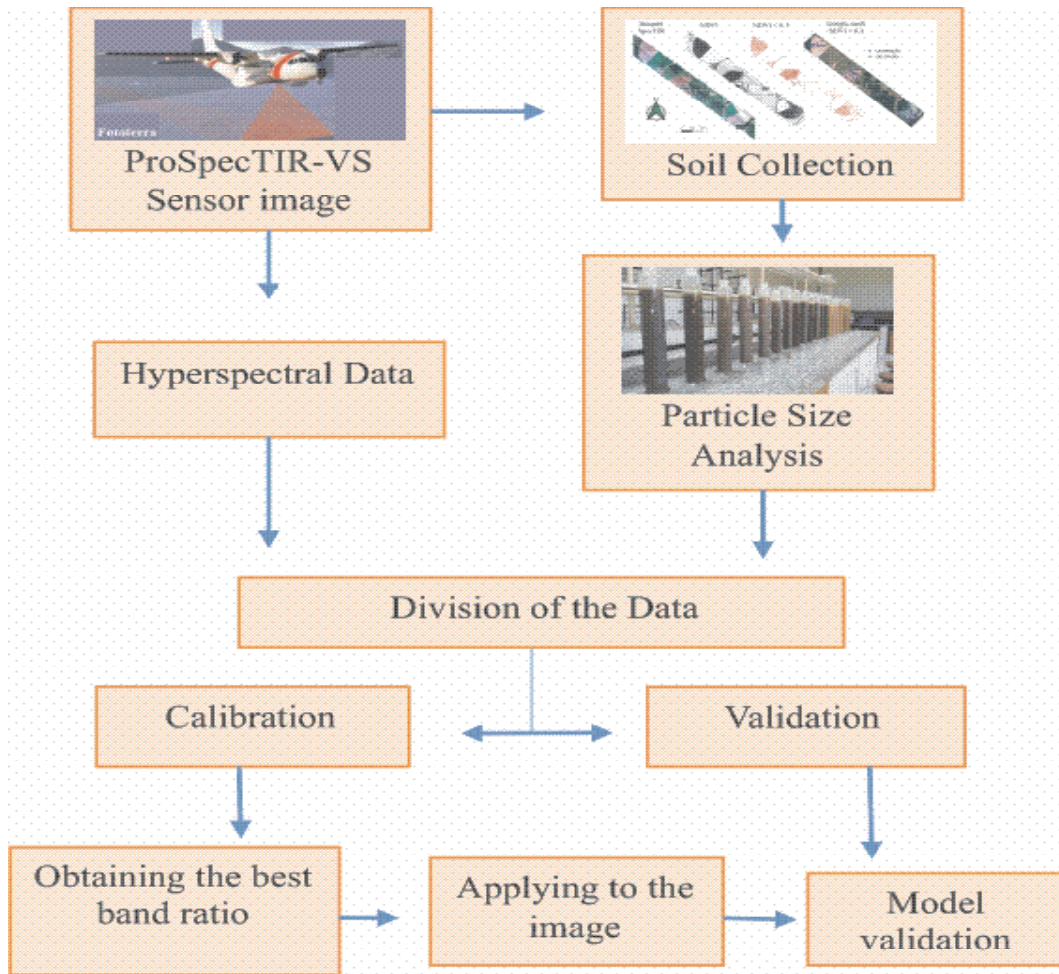
**Figure 2** - Location of the soil sampling points



The soil samples were divided, with 80% used to obtain the prediction model and 20% for

validation, as per the methodological flowchart shown in Figure 3.

Figure 3 - Methodological flowchart



**Data analysis**

A descriptive analysis of the sand, silt and clay content was carried out: mean, median, mode, standard error of the mean, minimum and maximum values, standard deviation, variance, coefficient of variation, kurtosis and asymmetry. All classical statistics, graphs and tables were obtained using the Microsoft Office® spreadsheet software.

A frequency distribution analysis of the attributes was made, together with a test for normality using the Kolmogorov-Smirnov test at 5%. This considers a null hypothesis for a sample taken from a normal population. To analyse the relationship between the spectral data and the sand and clay content, Pearson’s correlation was applied, as per Equation (1).

$$r = \frac{N \times \sum_{i=1}^N (Y_{c_i} - Y_{o_i})^2 - \sum_{i=1}^N Y_{o_i} \times \sum_{i=1}^N Y_{c_i}}{\sqrt{[N \times \sum_{i=1}^N Y_{o_i}^2 - (\sum_{i=1}^N Y_{o_i})^2] \times [N \times \sum_{i=1}^N Y_{c_i}^2 - (\sum_{i=1}^N Y_{c_i})^2]}} \quad (1)$$

where, r is Pearson’s correlation coefficient, Yc is the calculated value, Yo is the observed value and N the number of samples.

**Preparation of the Normalised Difference Index**

To build the Normalised Difference Index (NDI), all possible band ratios were tested in search of one that might estimate the texture of analysed soils with greater precision, as in Equation (2).

$$NDI = \frac{\rho_j - \rho_i}{\rho_j + \rho_i} \quad (2)$$

where, ρj and ρi are the reflectance of any two wavelengths within the 357 bands of the spectrum, and where i ≠ j.

The index was chosen based on the best coefficient of determination (R<sup>2</sup>) [Equation (3)] between the value obtained by the index and the sand or clay content determined in the laboratory. The calculations were made using a routine from the MatLab software. In order to

visualise the  $R^2$  values, contour maps were prepared by interpolation, employing the nearest neighbor method.

$$R^2 = \frac{\sum_{i=1}^N (Yc_i - \bar{Yc})^2}{\sum_{i=1}^N (Yo_i - \bar{Yo})^2} \quad (3)$$

where,  $Yc$  is the calculated value,  $Yo$  is the observed value and  $N$  is the total number of samples.

## RESULTS AND DISCUSSION

### Analysis of the textural data and descriptive statistics

**Figure 4** - Soil textural triangle (a) and sample-point distribution by texture (b)

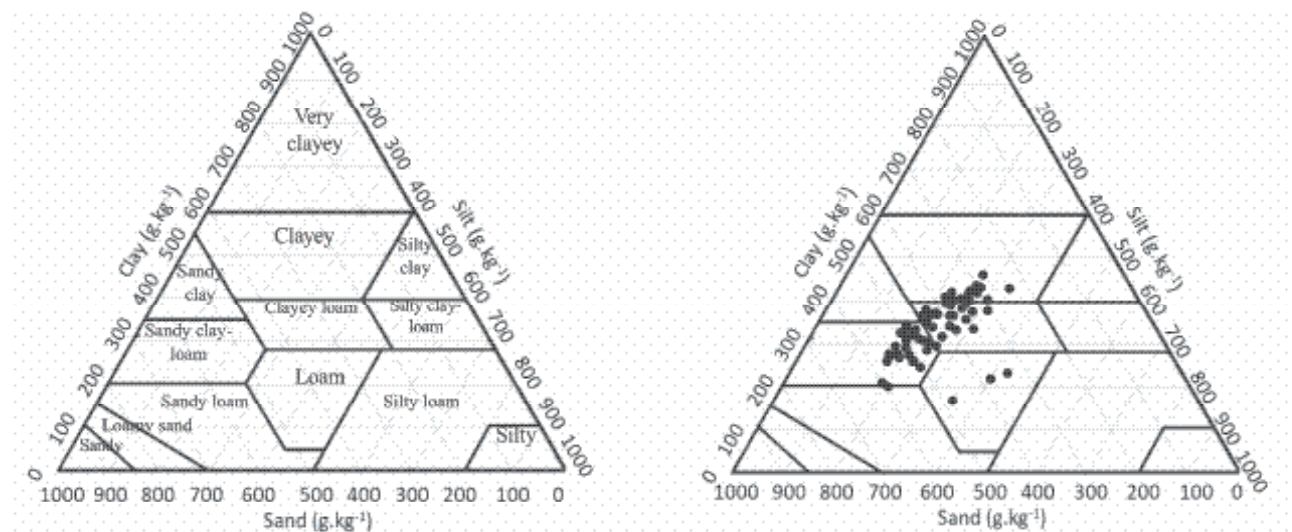


Figure 4 shows the textural classification of the 64 soil samples, where 40.6% were classified in the sandy clay-loam texture class, 34.4% were classified as clayey loam, 20.3% as clayey and 4.7% as having a loamy texture.

Table 1 shows the descriptive statistics for the sand, silt and clay content of the 64 soil samples. Among the fractions, the highest values for mean, variance and standard deviation were obtained for the sand content. The mean and median of the sand and clay values are close, indicating symmetrical distribution, which can be confirmed by the values for asymmetry being close to zero.

**Table 2** – Descriptive statistics for the sand, silt and clay content of the 64 soil samples

Descriptive statistics	Sand	Silt	Clay
	g.kg <sup>-1</sup>		
Mean	422.8	240.5	336.6
Standard error	10.8	6.5	8.2
Median	427.1	232.8	338.0
Standard deviation	86.8	52.3	65.2
Sample variance	7529.9	2735.4	4251.8
Coefficient of variation	20.52	21.74	19.37
Kurtosis	-0.9	2.6	-0.5
Asymmetry	0.0	1.3	-0.4
Amplitude	361.0	258.8	287.6
Minimum	236.9	171.5	169.9
Maximum	597.9	430.2	457.4
K-Smirnov (P-values)	0.6	0.5	0.7
Normality	Normal	Normal	Normal

The coefficient of asymmetry and kurtosis is more sensitive to extreme values than are the mean or standard deviation, since a single value can strongly influence these coefficients (ISAAKS; SRIVASTAVA, 1989). This can especially be seen in the values for silt (Table 2), which registered the greatest asymmetry.

### Analysis of the spectral data

Figure 5 shows the mean, standard deviation, maximum and minimum values for reflectance at all wavelengths, as obtained by the ProSpecTir-VS airborne sensor. The low reflectance values can be explained by the interaction between the radiation and atmospheric and environmental factors such as humidity and soil structure. As determined by Dewitte *et al.* (2012), the humidity and roughness of the soil surface reduce reflectance, since these are the main factors to influence backscatter radiation.

Pearson's correlation between the sand and clay content and soil reflectance (Figure 6) achieved the best results between 400 and 1350 nm, particularly in the 660 nm region, with correlation values reaching 0.30. The wavelength that most correlated with the sand content was 662 nm, showing a negative correlation. For clay, the best result was at 658 nm, with a positive correlation.

The low correlation (Figure 6) between the mineral particles of the soil and reflectance, can be explained by the spectral mixture, with interference in soil surface reflectance coming mainly from the gravel, as well as by the mineralogy of this gravel in the study region, which is composed mainly of nodules and ferruginous concretions (GIRÃO *et al.*, 2014). The gravel in the soil samples ranged from 56 to 171 g kg<sup>-1</sup>. This is an indication that the spectral response of the soils, obtained by the ProSpecTIR-VS sensor, may have been

influenced by the surface roughness and mineralogy of the gravel, resulting in a decrease in reflectance. The nodules and concretions, also found on the surface, are ferruginous, with oxidic mineralogy, especially hematite and goethite, and the presence of kaolinite as the main phyllosilicate (GIRÃO *et al.*, 2014; MOTA *et al.*, 2007).

Spectral mixing can occur when the materials are smaller than the dimensions of the pixel; as such, the radiation flow detected by the sensor is composed of a mixture of radiation from all the materials within the pixel (SHIMABUKURO; PONZONI, 2017).

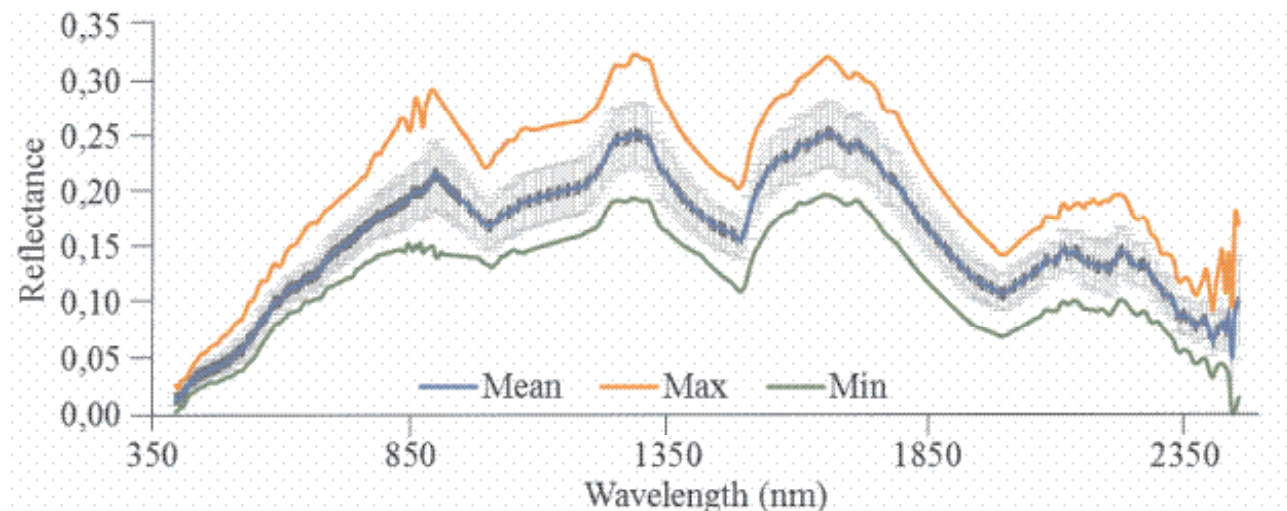
Figure 7 plots the spectra of the most sandy and clayey soil samples. In general, sandy soils tend to have greater reflectance due to their mineralogical composition (rich in quartz); whereas in medium to clayey soils the opposite occurs, as underlined by Cezar *et al.* (2012). However, with the soil samples in this research, the loamiest soil was characterised by greater reflectance than the sandy soil, as shown in Figure 7.

This is probably due to the soils of the study region containing nodules and ferruginous concretions (GIRÃO *et al.*, 2014), and also to the size of the sand, with the sandy soil, therefore, reflecting less than the clayey soil. Cezar *et al.* (2012), when comparing the reflectance factor of sand with and without the presence of iron oxide, observed the ability of iron oxides to absorb electromagnetic energy.

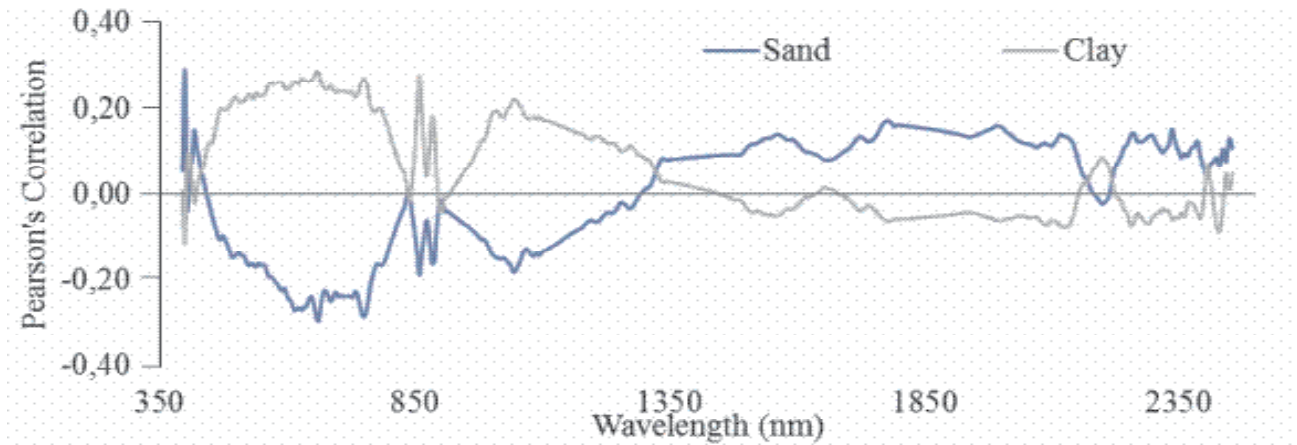
### Normalised Difference Index - NDI

Figure 8 shows a plot of the Coefficients of Determination ( $R^2$ ) between the results of the indices, using the spectra obtained with the ProSpecTIR-VS sensor, and the sand and clay content. The best results for  $R^2$  were found in

**Figure 5** - Mean (blue line), standard deviation (grey border), maximum (orange line) and minimum (green line) for reflectance at the different wavelengths in the 64 soil samples, obtained by the ProSpecTIR-VS sensor



**Figure 6** - Pearson's correlation between the sand and clay content and reflectance of the soil samples



**Figure 7** - Spectral response of two soil samples with different texture

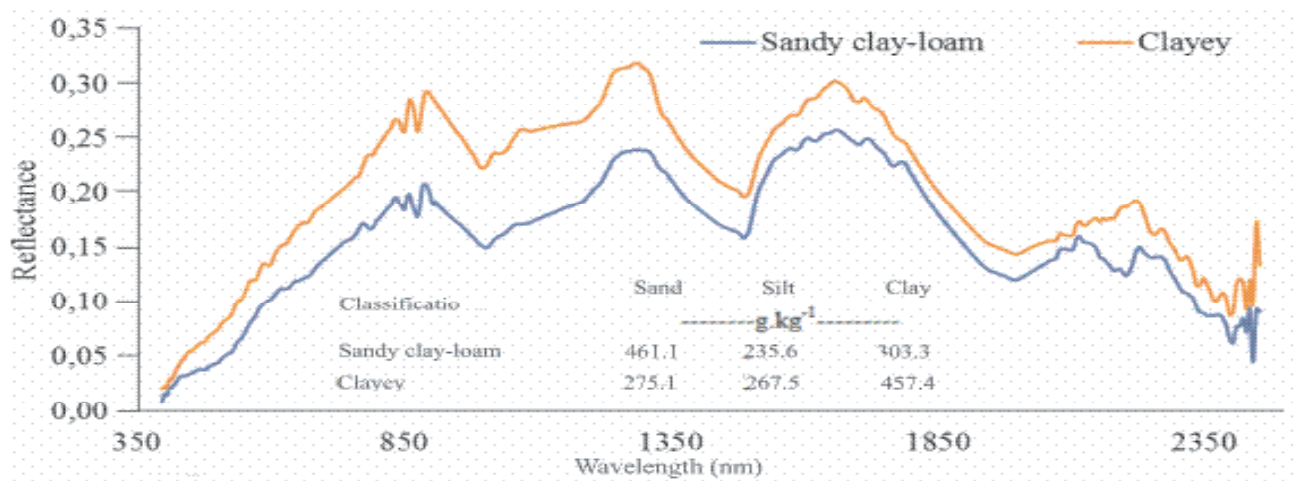
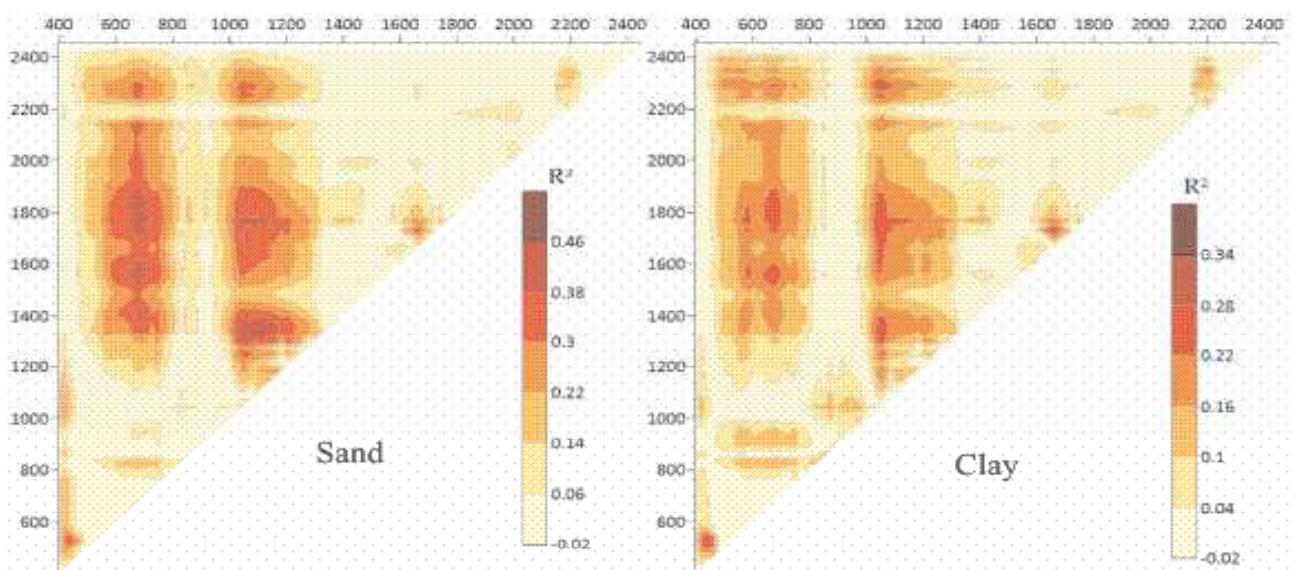


**Figure 8** - Coefficient of Determination ( $R^2$ ) between the NDI of the spectral data and the sand and clay content



the estimate for sand, especially when the band ratio involved wavelengths around 1050 and 1300 nm, as well as around 600 and 1800 nm, as also shown in Table 3. These bands may be related to humidity (1300 and 1800 nm) and the presence of iron oxides (600 and 1050 nm); bands close to these were also seen by Genú and Demattê (2012) and Demattê *et al.* (2015).

The model for estimating sand using the NDI in bands 1045 and 1323 can be seen in Figure 9, where the Coefficient of Determination was 0.50.

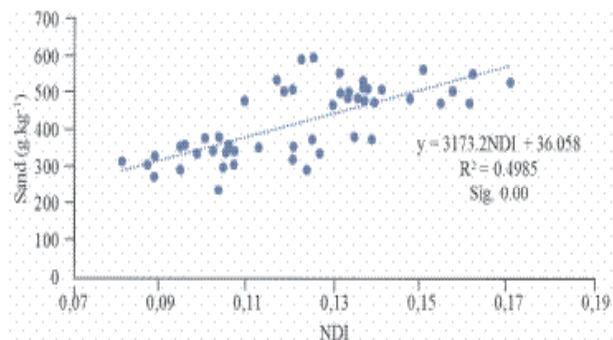
To validate the model, the coefficient of determination ( $R^2$ ) was obtained between the estimated and measured values for sand in the 20% of samples not used for calibration. Figure 10a shows the ratio between the measured sand content and that estimated by the model from Figure 9. Among the validation samples, an outlier can be seen in the graph in Figure 10a, which caused a reduction in  $R^2$  from 0.84 to 0.45, as well as an increase in the RMSE from 3.71 to 4.29, considering the value outside the curve when compared with Figure 10b.

After applying the NDI to the ProSpecTIR-VS hyperspectral images to pixels with exposed soil only, the sand was estimated using the regression model shown

**Table 3** – The best NDIs for estimating sand and clay

Sand			Clay		
Band 1	Band 2	$R^2$	Band 1	Band 2	$R^2$
1045	1323	0.50	1667	1717	0.40
1052	1323	0.49	1661	1717	0.38
1045	1317	0.49	1667	1724	0.38
1045	1329	0.49	1655	1724	0.37
662	1774	0.49	1661	1724	0.37
662	1780	0.49	1649	1724	0.36

**Figure 9** – Model for estimating sand, using the NDI comprising the 1045 and 1323 nm bands



in Figure 9. This generated the map shown Figure 11, resulting in 82.1% of the pixels with values between 200 and 600  $g.kg^{-1}$  sand, falling between the minimum and maximum sand content of the soil samples. It is important to note that 41% of the pixels had a sand content close to the mean value of the soil samples (Table 1).

**Figure 10** - Ratio between the measured and estimated sand content (a) and without the outlier (b)

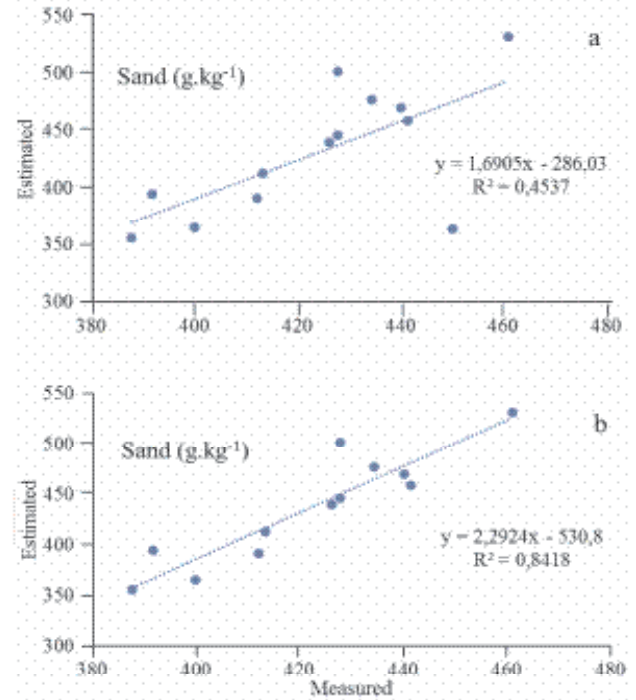
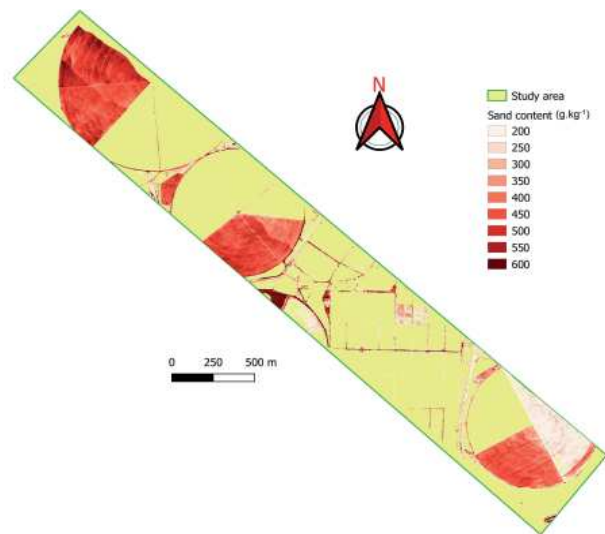


**Figure 11** - Map of the sand content



In the generated map (Figure 11), a reduction in sand content can be seen from northwest to southeast, which indicates a spatial dependence of the attribute. It is worth pointing out that outliers were found in the spectral response of the soil, but this is due to the presence of materials on the soil surface, such as invasive plants and crop stubble.

## CONCLUSIONS

1. It was concluded that it is possible to build a Normalised Difference Index using data from the ProSpecTIR-VS sensor in bands 1045 and 1323, capable of estimating textural attributes, especially the sand content of the soil, with an  $R^2$  value of 0.50;
2. In addition, the NDI was applied to the image obtained by the ProSpecTIR sensor, which enabled the construction of a sand map that could then serve as a basis for decision making by irrigators in the Jaguaribe-Apodi irrigated perimeter.

## ACKNOWLEDGMENTS

The authors of this study would like to thank the Instituto Nacional de Ciência e Tecnologia em Salinidade - INCTSal and the Conselho Nacional de Desenvolvimento Científico e Tecnológico - CNPQ for making it possible to acquire Hyperspectral images from the SpecTIR-VS sensor.

## REFERENCES

- AGÊNCIA DE DESENVOLVIMENTO DO ESTADO DO CEARÁ. **Perímetros públicos irrigados do Ceará**. Fortaleza: ADECE, 2011. 20 p.
- AMARAL, C. H. do. *et al.* Characterization of indicator tree species in neotropical environments and implications for geological mapping. **Remote Sensing of Environment**, v. 216, p. 385-400, 2018.
- AMARAL, C. H. do. *et al.* Mapping invasive species and spectral mixture relationships with neotropical woody formations in southeastern Brazil. **ISPRS Journal of Photogrammetry and Remote Sensing**, v. 108, p. 80-93, 2015.
- BRADY, N. C.; WEIL, R. R. **Elementos da natureza e propriedades dos solos**. 3. ed. Porto Alegre: Bookman, 2013. 704 p.
- CASA, R. *et al.* A comparison of sensor resolution and calibration strategies for soil texture estimation from hyperspectral remote sensing. **Geoderma**, v. 197/198, p. 17-26, 2013.
- CASTALDI, F. *et al.* Estimation of soil properties at the field scale from satellite data: a comparison between spatial and non-

spatial techniques. **European Journal of Soil Science**, v. 65, n. 6, p. 842-851, November 2014.

CASTALDI, F. *et al.* Evaluation of the potential of the current and forthcoming multispectral and hyperspectral imagers to estimate soil texture and organic carbon. **Remote Sensing of Environment**, v. 179, p. 54-65, 2016.

CEZAR, *et al.* Avaliação e quantificação das frações silte, areia e argila por meio de suas respectivas reflectâncias. **Revista Brasileira de Ciência do Solo**, v. 36, n. 4, p. 1157-1165, 2012.

DEMATTÊ, J. A. M. *et al.* Espectroscopia VIS-NIR-SWIR na avaliação de solos ao longo de uma toposequência em Piracicaba (SP). **Revista Ciência Agronômica**, v. 46, n. 4, 2015.

DEWITTE, O. *et al.* Satellite remote sensing for soil mapping in Africa: an overview. **Progress in Physical Geograph**, v. 36, n. 4, p. 514-538, 2012.

GATTO, L. C. S. **Diagnóstico ambiental da Bacia do Rio Jaguaribe: diretrizes gerais para a ordenação territorial**. Salvador: IBGE, 1999. 77 p.

GENÚ, A. M.; DEMATTÊ, J. A. M. Espectrorradiometria de solos e comparação com sensores orbitais. **Bragantia**, v. 71, n. 1, p. 82-89, 2012.

GIRÃO, R. O. *et al.* Soil genesis and iron nodules in a karst environment of the Apodi Plateau. **Revista Ciência Agronômica**, v. 45, n. 4, p. 683-695, 2014.

ISAAKS, E. H.; SRIVASTAVA, R. M. **An introduction to applied geostatistics**. New York: [s. n.], 1989. 561 p.

JACOMINE, P. K. T.; ALMEIDA, J. C.; MEDEIROS, L. A. R. **Levantamento exploratório: reconhecimento de solos do Estado do Ceará**. Recife: Embrapa: DPP: Sudene, 1973. v. II, 830 p. (Boletim Técnico, 28. Série Pedológica, 16).

LIAO, K. *et al.* Spatial estimation of surface soil texture using remote sensing data. **Soil Science and Plant Nutrition**, v. 59, n. 4, p. 488-500, 2013.

MOTA, J. C. A. *et al.* Atributos mineralógicos de três solos explorados com a cultura do melão na Chapada do Apodi - RN. **Revista Brasileira de Ciência do Solo**, v. 31, n. 3, p. 445-454, 2007.

NANNI, M. R.; DEMATTÊ, J. A. M. Comportamento da linha do solo obtida por espectrorradiometria laboratorial para diferentes classes de solo. **Revista Brasileira de Ciência do Solo**, v. 30, n. 6, p. 1031-1038, 2006. RIBEIRO, G. A.; SILVA, J. N. C.; SILVA, J. B. Índice de Vegetação Ajustado ao Solo (IVAS): estado da arte e suas potencialidades. **Revista Brasileira de Geografia Física**, v. 9, n. 6, p. 2054-2074, 2016.

ROCHA NETO, O. C. *et al.* Hyperspectral remote sensing for detecting soil salinization using ProSpecTIR-VS aerial imagery and sensor simulation. **Remote Sensing**, v. 9, n. 42, p. 1-16, 2017.

SANCHES, I. D.; SOUZA FILHO, C. R.; KOKALY, R. F. Spectroscopic remote sensing of plant stress at leaf and canopy levels using the chlorophyll 680 nm absorption feature with continuum removal. **ISPRS Journal of Photogrammetry and Remote Sensing**, v. 97, p. 111-122, 2014.

SHIMABUKURO, Y. E.; PONZONI, F. J. **Mistura espectral: modelo linear e aplicações.** São Paulo: Oficina de Textos, 2017. 127 p.

STREHER, A. S. *et al.* Sunlint correction in airborne hyperspectral images over inland waters. **Revista Brasileira de Cartografia**, v. 66, n. 7, p. 1437-1449, 2014.

TEIXEIRA, P. C. *et al.* **Manual de métodos de análise de solo.** 3. ed. Brasília: Embrapa, 2017.

VIÑA, A. *et al.* Comparison of different vegetation indices for the remote assessment of green leaf area index of crops. **Remote Sensing of Environment**, v. 115, n. 12, p. 3468-3478, 2011.